Published in final edited form as:
Am J Physiol Renal Physiol. 2008 April ; 294(4): F937–F944. doi:10.1152/ajprenal.00591.2007.

Increased renal renin content in mice lacking the Na^+/H^+ exchanger NHE2

Fiona Hanner[1], **Régine Chambrey**[2], **Soline Bourgeois**[2], **Elliott Meer**[1], **István Mucsi**[3,4], **László Rosivall**[3,5], **Gary E. Shull**[6], **John N. Lorenz**[7], **Dominique Eladari**[2,8], and **János Peti-Peterdi**[1,3]

[1]Departments of Physiology and Biophysics and Medicine, Zilkha Neurogenetic Institute, University of Southern California, Los Angeles, California

[2]Institut National de la Santé et de la Recherche Médicale Unité 872, Centre de Recherche des Cordeliers and Faculté de Medecine René Descartes, Université Paris V, Paris

[3]Hungarian Academy of Sciences, Semmelweis University Research Group for Pediatrics and Nephrology, Semmelweis University, Budapest, Hungary

[4]1st Department of Medicine, Semmelweis University, Budapest, Hungary

[5]Institute of Pathophysiology, Faculty of Medicine, Semmelweis University, Budapest, Hungary

[6]Departments of Molecular Genetics, Biochemistry, and Microbiology, University of Cincinnati College of Medicine, Cincinnati, Ohio

[7]Department of Molecular and Cellular Physiology, University of Cincinnati College of Medicine, Cincinnati, Ohio

[8]Département de Physiologie, Hôpital Necker-Enfants Malades, Paris, France

Abstract

Macula densa (MD) cells express the Na^+/H^+ exchanger (NHE) isoform NHE2 at the apical membrane, which may play an important role in tubular salt sensing through the regulation of cell volume and intracellular pH. These studies aimed to determine whether NHE2 participates in the MD control of renin synthesis. Renal renin content and activity and elements of the MD signaling pathway were analyzed using wild-type ($NHE2^{+/+}$) and NHE2 knockout ($NHE2^{-/-}$) mice. Immunofluorescence studies indicated that $NHE2^{-/-}$ mice lack NHE3 at the MD apical membrane, so the other apical NHE isoform has not compensated for the lack of NHE2. Importantly, the number of renin-expressing cells in the afferent arteriole in $NHE2^{-/-}$ mice was increased ~2.5-fold using renin immunohistochemistry. Western blotting confirmed ~20% higher renal cortical renin content in $NHE2^{-/-}$ mice compared with wild type. No-salt diet for 1 wk significantly increased renin content and activity in $NHE2^{+/+}$ mice, but the response was blunted in $NHE2^{-/-}$ mice. Renal tissue renin activity and plasma renin concentration were elevated three- and twofold, respectively, in $NHE2^{-/-}$ mice compared with wild type. $NHE2^{-/-}$ mice also exhibited a significantly increased renal cortical cyclooxygenase-2 (COX-2) and microsomal prostaglandin E synthase (mPGES) expression, indicating MD-specific mechanisms responsible for the increased renin content. Significant and chronic activation of ERK1/2 was observed in MD cells of $NHE2^{-/-}$ kidneys. Removal of salt or addition of NHE inhibitors to cultured mouse MD-derived (MMDD1) cells caused a time-dependent activation of ERK1/2. In conclusion, the NHE2 isoform appears to be important in the MD feedback control of renin secretion, and the signaling

Address for reprint requests and other correspondence: J. Peti-Peterdi, Univ. of Southern California, Zilkha Neurogenetic Institute, 1501 San Pablo St., ZNI 335, Los Angeles, CA 90033 (petipete@usc.edu).

pathway likely involves MD cell shrinkage and activation of ERK1/2, COX-2, and mPGES, all well-established elements of the MD-PGE_2-renin release pathway.

Keywords

macula densa; cell volume; renin release; mitogen-activated protein kinases; cyclooxygenase-2

The juxtaglomerular apparatus (JGA) represents a major structural component of the renin-angiotensin system and is one of the most important regulatory sites of renal salt and water conservation and blood pressure maintenance (36,37). The JGA consists of a tubular component (the macula densa, MD), the extraglomerular mesangium, and a vascular component that includes the terminal part of the afferent arteriole containing the renin-producing juxtaglomerular (JG) cells (2). Two major regulatory functions are performed by the JGA: the high distal tubular NaCl concentration ([NaCl])-induced afferent arteriolar vasoconstriction (tubuloglomerular feedback, TGF) and the low tubular [NaCl]-induced renin release (3,5,22,23,36–38,41). MD cells are strategically positioned in the JGA with their apical membrane exposed to the tubular fluid, while their basilar aspects are in contact with cells of the mesangium and the afferent arteriole (2,3).

The MD plaque is a unique group of 15–20 cells located at the end of the cortical thick ascending limb in close association with the JGA-glomerulus complex. These cells play a pivotal role in sensing changes in luminal fluid composition, generating and sending signals to the JGA that control renal blood flow and glomerular filtration rate and renin release (36,37). Tubular salt sensing by the MD has been shown to involve apical NaCl transport mechanisms including the furosemide-sensitive Na^+-K^+-$2Cl^-$ cotransporter (NKCC2), which is considered the primary NaCl entry mechanism (3,22,23,36–38). In fact, a classic hallmark of the TGF and renin release mechanisms is their effective inhibition by furosemide or other loop diuretics (3,5,22,23,36–38). The downstream elements of MD-mediated renin release signaling include, at least, the low tubular salt-induced activation of p38 and ERK1/2 MAP kinases, cyclooxygenase-2 (COX-2), and microsomal prostaglandin E synthase (mPGES) in the MD (8,9,15,34,45) and the synthesis and release of PGE_2 (34). PGE_2 acts on JG cells' EP2 and EP4 receptors and causes renin release (40,41).

Besides the well-known NKCC2, MD cells possess an apical Na^+/H^+ exchanger (NHE) that may also participate in Na^+ transport as well as in the regulation of cell volume and intracellular pH (pH_i) in these cells (10,31). This exchanger was identified as the NHE2 isoform (31). Interestingly, MD cells also possess the basolateral Na^+/H^+ exchanger NHE4 (31). This polarized NHE2/NHE4 configuration in the MD is unique and distinct from the usual NHE3/NHE1 arrangement in other nephron segments (1), suggesting that NHEs may play an important role in MD cell function. Accordingly, MD apical NHE activity, through its effect on pH_i, was shown to regulate neuronal nitric oxide synthase and modulate TGF responses, at least in vitro (20,43). A recent study, however, showed that TGF responses under control conditions were not different in NHE2-deficient mice compared with wild type (24). The present studies aimed to determine whether NHE2 participates in the MD control of renin synthesis and release.

Materials and Methods

Animal breeding and genotyping

The generation and characterization of $NHE2^{-/-}$ mice have been reported (19,39). Heterozygotes were obtained from an established colony and bred to produce NHE2 wild-type ($NHE2^{+/+}$) and null ($NHE2^{-/-}$) mice. All mice were genotyped at the age of 3 wk by

PCR, using DNA from tail biopsies as previously described (19), using the following primers: NHE2-wild type (wt) forward, 5′-CATCTCTATCACAAGTTGCCCACAATCGTG-3′; NHE2-wt reverse, 5′-GTGACTGCATCGTTGAGCAGAGACTCG-3′; and NHE2-mutant (mt), 5′-GACAATAGCAGGCATGCTGG-3′. Mice were fed standard chow (0.3% NaCl) or salt-deficient diet (113760; Dyets, Bethlehem, PA) for 1 wk. Wild-type and null mice were age matched in all experiments. All animal protocols were approved by the Institutional Animal Care and Use Committee at the University of Southern California and the University of Paris.

Antibodies

Two different renin antibodies were used. One rabbit anti-mouse renin antibody was a kind gift from Dr. Inagami (Vanderbilt University, Nashville, TN), and the other was purchased from Dr. E. J. Brandt (Technology Transfer Office, St. Louis University, St. Louis, MO). A rabbit polyclonal antibody against mPGES was purchased from Cayman Chemical (Ann Arbor, MI). The goat polyclonal COX-2 and actin antibodies were purchased from Santa Cruz Biotechnology (Santa Cruz, CA). A monoclonal GAPDH antibody was purchased from Ambion (Austin, TX). A rabbit polyclonal anti-phosphorylated ERK1/2 (pERK1/2) antibody was purchased from Cell Signaling Technology (Danvers, MA). The NHE3 antibody was purchased from Chemicon (Temecula, CA). These antibodies have been previously characterized (4,11,27,34,35,45).

Immunofluorescence labeling of kidney tissue

Mice were anesthetized with 100 mg/kg Inactin, and their kidneys were fixed in situ by perfusion of 4% paraformaldehyde in PBS. Coronal kidney sections were then post-fixed overnight at 4°C in 4% paraformaldehyde and embedded in paraffin. Subsequently, 5-μm sections of the paraffin block were deparaffinized in toluene and rehydrated through graded ethanol. To retrieve antigens and enable immunostaining on paraformaldehyde-fixed paraffin-embedded tissue, the sections were heated in PBS in a microwave for 20 min (boiling) and then allowed to cool in the PBS for 40 min. To reduce nonspecific binding, sections were blocked for 30 min with 20% normal goat serum in PBS. Sections were then incubated with the NHE3 or renin or with pERK1/2 antibodies at a dilution of 1:100 for 1 h. Sections were labeled with an Alexa Fluor 594-conjugated goat anti-rabbit antibody (Molecular Probes, Eugene, OR) for 1 h at a dilution of 1:500. After a wash step, sections were mounted with Vectashield mounting medium containing the nuclear stain 4,6-diamidino-2-phenylindole (Vector Laboratories) and examined with a Leica TCS SP2 confocal microscope. All sections were labeled in parallel.

Measuring tissue renin activity

Renin activity of homogenized renal cortical tissue was measured using a fluorescence resonance energy transfer (FRET)-based 5-[(2-aminoethyl)amino]naphthalene-1-sulfonic acid (EDANS)-conjugated renin substrate (Anaspec, San Jose, CA) and a cuvette-based spectrofluorometer (Quantamaster-8; PTI, Birmingham, NJ) as described previously (16,35). Briefly, 2 μM of the renin substrate in a solution of 200 mM NaCl and 50 mM Tris adjusted to pH 8.0 was loaded into the cuvette and heated to 37°C. After a baseline reading was taken, 100-μg homogenized kidney tissue samples were mixed with the renin substrate in the 37°C chamber, and the emitted fluorescence signal as an index of ANG I generation was measured at 490 nm in response to excitation at 340 nm for a period of 500 s. The initial rate of the increase in EDANS fluorescence was then analyzed as a measure of renin activity using FeliX32 software (PTI).

Measuring plasma renin concentration

Plasma renin concentration (PRC) was measured by radioimmunoassay of ANG I generated by incubating the plasma at pH 8.5 in the presence of an excess of rat angiotensinogen as previously described (26).

Cell culture

Mouse macula densa-derived (MMDD1) cells were a kind gift of Dr. Jürgen Schnermann (National Institutes of Health, Bethesda, MD). These cells were successfully used before to study the activation of p38 and ERK1/2 MAP kinases, well-established elements of the MD renin release signal, by using various physiological stimuli, including isosmotic reduction of medium Cl^- concentrations (45). MMDD1 cells were cultured as described previously (45).

RT-PCR

Total RNA was purified from whole mouse kidney samples or confluent MMDD1 cells by using a Total RNA mini kit in accordance with the manufacturer's instructions (Bio-Rad, Hercules, CA). RNA was then quantified using spectrophotometry and reverse-transcribed to single-stranded cDNA using avian reverse transcriptase and random hexamers according to the manufacturer's instructions (Thermoscript RT-PCR system; Invitrogen). cDNA (2 μl) was amplified using a master mix containing *Taq* polymerase (Invitrogen) and the following primers: NHE2-wt forward and NHE2-wt reverse (listed above), β-actin sense, 5′-GGTGTGATGGTGGGAATGGGTC-3′, and β-actin antisense, 5′-ATGGCGTGAGGGAGAGCATAGC-3′ as published earlier (25), each at a final concentration of 200 μM. The PCR reaction was carried out for 45 cycles of 94°C for 30 s, 60°C for 30 s, and 72°C for 30 s. The PCR product was analyzed on a 2% agarose gel stained with ethidium bromide to identify fragments of ~455 bp for NHE2 and 350 bp for β-actin.

Western blotting

Mice were anesthetized with 100 mg/kg Inactin, and kidneys were removed. Slices of cortex were manually dissected, and tissue was homogenized with a rotor-stator homogenizer in a buffer containing 20 mM Tris·HCl, 1 mM EGTA, pH 7.0, and a protease inhibitor cocktail (BD Bioscience, San Jose, CA). Samples were centrifuged at low speed to pellet cellular debris, and supernatant was collected and assayed for protein concentration by using a modified Bradford method (Quick Start Bradford protein assay; Bio-Rad). Forty micrograms of protein were run per lane, separated on either a 7.5 or 4–20% SDS-polyacrylamide gel, depending on the protein of interest. The samples were then transferred to a polyvinylidene difluoride membrane (Bio-Rad). After the membrane was blocked in 5% nonfat dry milk, immunoblotting was performed with a polyclonal antibody to renin (1:250 dilution), a rabbit polyclonal antibody to mPGES (1:200 dilution), or a goat polyclonal COX-2 antibody (1:200 dilution). Reactivity was detected using a horseradish peroxidase-labeled goat anti-rabbit (1:1,000 dilution; Santa Cruz Biotechnology) or donkey anti-goat secondary antibody (1:1,000 dilution; Santa Cruz Biotechnology). An enhanced chemiluminescence kit (Amersham Biosciences, Little Chalfont, UK) was used to visualize the secondary antibody. The blot was stripped and reprobed with a goat polyclonal antibody to actin (1:200 dilution; Santa Cruz Biotechnology) to test for protein loading and quality of transfer.

MMDD1 cells were grown to confluence on plates as previously described (45). In some experiments, the cells bathed in Krebs-Ringer solution were incubated with a NaCl-free isosmotic, modified Krebs-Ringer solution [NaCl was replaced with *N*-methyl-D-glucamine cyclamate as described previously (31)], 100 μM furosemide, 100 μM dimethyl amiloride (DMA) or 100 μM ethylisopropyl amiloride (EIPA), 20 mM NH_4Cl, 10 μM nigericin, or

500 mosmol/kgH_2O modified Krebs-Ringer solution (by adding mannitol) for 0, 2, 5, or 15 min. All reagents were purchased from Sigma. After treatment, cells were lysed using CellLytic-M lysis buffer (Sigma) according to the manufacturer's instructions and centrifuged at maximum speed for 20 min. The supernatant was collected and assayed as previously described. Samples were run on 4–20% gels and probed with anti-pERK1/2 antibodies overnight at a dilution of 1:500 and imaged as described above. Blots were then probed for 1 h with GAPDH (1:4,000; Ambion), which served as a loading control.

Densitometric analysis of blots was performed using National Institutes of Health ImageJ software. The data were then normalized against the control sample, and an average for each group was calculated.

The pH_i of MMDD1 cells in culture was measured using the pH-sensitive fluorophore BCECF as described previously (31). Briefly, MMDD1 cells grown on glass coverslips were loaded with the dye by adding 10 μM BCECF-AM to the culture medium at 37°C. Coverslips were inserted in a cuvette-based spectrofluorometer (Quantamaster-8; PTI) and superfused with Krebs-Ringer solution containing either 20 mM NH_4Cl (alkalinization) (45) or 10 μM nigericin (cell acidification) (30). BCECF fluorescence was detected continuously (5 points/s) at 530 nm in response to excitation at 500 and 440 nm. pH_i was determined as the excitation ratio signal (500 nm/440 nm).

Cell volume changes of MMDD1 cells in culture were measured using fluorescence detection of calcein self-quenching as described previously (14). Briefly, MMDD1 cells were incubated with 10 μM calcein-AM as described above for BCECF. Calcein was excited at 490 nm, and fluorescence was detected at 530 nm. The coverslip-containing cuvette was superfused with Krebs-Ringer solution, and after calcein fluorescence stabilized, the cells were superfused with either 500 mosmol/kgH_2O modified Krebs-Ringer solution (by adding mannitol) or isosmotic Krebs-Ringer solution containing 100 μM EIPA. Reduction in cell volume was detected by decreased calcein fluorescence due to cell shrinkage-induced concentration and self-quenching of the dye.

Data analysis

Statistical significance was tested using an unpaired *t*-test assuming equal variance. Plasma renin concentration was analyzed using the Mann-Whitney test. Data are means ± SE. Significance was accepted at $P < 0.05$.

Results

Renin immunohistochemistry

Kidneys from $NHE2^{+/+}$ (Fig. 1A) and $NHE2^{-/-}$ mice (Fig. 1B) were paraffin-embedded, sectioned, and stained in parallel with a renin antibody. Intense renin immunolabeling was detected in cells of the terminal JG segment of afferent arterioles in both $NHE2^{+/+}$ and $NHE2^{-/-}$ mice. Importantly, the number of positively labeled renin-producing JG cells per afferent arteriole was ~2.5-fold higher in $NHE2^{-/-}$ compared with $NHE2^{+/+}$ mouse kidneys (Fig. 1C). The average number of JG cells per afferent arteriole was 3.2 ± 0.5 in $NHE2^{+/+}$ and 7.6 ± 0.6 in $NHE2^{-/-}$ kidneys ($P < 0.05$, the number of afferent arterioles analyzed was $n = 10$ in the $NHE2^{-/-}$ and $n = 5$ in the $NHE2^{+/+}$ group from 5 separate kidneys in each group).

Renin immunoblotting

Renal cortical tissue samples were removed from $NHE2^{-/-}$ ($n = 6$) and $NHE2^{+/+}$ mice ($n = 5$) fed a control diet and immunoblotted for renin (Fig. 2A). Probing the blots with a

GAPDH antibody confirmed equal protein loading (Fig. 2A). The blots were then analyzed using densitometry (Fig. 2B). Renin expression was 20% higher in $NHE2^{-/-}$ mice compared with $NHE2^{+/+}$ mice on normal salt diet ($P < 0.05$). As expected, no-salt diet for 1 wk significantly increased renin content in $NHE2^{+/+}$ mice (2.3-fold), but this response was blunted in $NHE2^{-/-}$ mice (17% increase, $P < 0.05$; Fig. 2B).

Plasma and kidney tissue renin activity

Renal cortical tissue renin activity was assayed using spectrofluorometry. Tissue homogenates were prepared and mixed with the fluorogenic renin substrate and assay buffer. The emitted FRET signal, an index of ANG I generation (renin activity), was measured and plotted as a function of time (Fig. 3A) and quantified (Fig. 3B). Renin activity was threefold higher in the renal cortex from $NHE2^{-/-}$ compared with $NHE2^{+/+}$ mice ($NHE2^{+/+}$: 30.4 ± 6.6, $n = 5$; $NHE2^{-/-}$: 99.5 ± 16.2, $n = 6$, $P < 0.01$). No-salt diet for 1 wk increased renal tissue renin activity sixfold in $NHE2^{+/+}$ mice (179.8 ± 0.6, $P < 0.01$), but this response was significantly blunted in $NHE2^{-/-}$ mice (132.2 ± 33.9, not significantly different from $NHE2^{-/-}$ mice on normal diet; Fig. 2B).

To determine whether the higher intrarenal renin content and activity in $NHE2^{-/-}$ mice are reflected in the serum, we measured PRC in $NHE2^{-/-}$ ($n = 11$) and $NHE2^{+/+}$ mice ($n = 8$). PRC was significantly increased (Fig. 3C), more than twofold in $NHE2^{-/-}$ compared with $NHE2^{+/+}$ mice ($NHE2^{+/+}$: 0.83 ± 0.18 μg ANG $I \cdot h^{-1} \cdot ml^{-1}$; $NHE2^{-/-}$: 1.92 ± 0.68 μg ANG $I \cdot h^{-1} \cdot ml^{-1}$, $P < 0.05$).

NHE3 expression in $NHE2^{-/-}$ mice

To evaluate the possibility that the loss of NHE2 function in MD cells of $NHE2^{-/-}$ mice is compensated for by an increase in the other main apical NHE isoform NHE3, we analyzed expression of NHE3 using immunohistochemistry. Sections from $NHE2^{+/+}$ and $NHE2^{-/-}$ mouse kidneys were incubated with an NHE3 antibody and imaged. Similar to wild-type controls (Fig. 4A), $NHE2^{-/-}$ mice did not show any signs of NHE3 expression at the apical membrane of MD cells (Fig. 4B), whereas the adjacent cells of the thick ascending limb were labeled as in controls (Fig. 4, A and B).

Renal COX-2 and mPGES expression

To test whether the observed increases in renal renin content and activity in $NHE2^{-/-}$ mice are possibly due to MD-specific mechanisms, we compared the expression of renin, COX-2, and mPGES in the same homogenates of renal cortex using immunoblotting (Fig. 5). Expression levels were quantified by densitometry and then normalized to wild-type controls. Parallel with the increase in renal cortical renin content as established above, both COX-2 (1.62 ± 0.05) and mPGES expression (1.24 ± 0.05) were significantly increased in $NHE2^{-/-}$ mice compared with $NHE2^{+/+}$ (62 and 24% increases, respectively, $P < 0.05$).

MAPK activation in macula densa cells of $NHE2^{-/-}$ mice

Since the activation of ERK1/2 MAP kinases are well-established elements of the MD renin release signal (8,9,45), immunofluorescence studies were performed on $NHE2^{+/+}$ and $NHE2^{-/-}$ mouse kidney sections using a pERK1/2 antibody (Fig. 6). Specific immunolabeling was found in cells of the MD and the adjacent cortical thick ascending limb in both genotypes (Fig. 6, A and B). However, the number of positively labeled tubular epithelial cells per JGA was ~3.5-fold higher in $NHE2^{-/-}$ compared with $NHE2^{+/+}$ mice (Fig. 6C). The average number of pERK1/2-positive cells per JGA was 2.6 ± 0.4 in $NHE2^{+/+}$ and 9.0 ± 0.9 in $NHE2^{-/-}$ kidneys ($P < 0.05$).

MAPK activation in MMDD1 cells

This series of experiments was performed to further identify the NHE2- and ERK1/2-dependent cellular mechanism that causes the activation of the MD renin release signal. After confirming that the MMDD1 cells express NHE2 (Fig. 7A), we studied the effects of low NaCl and ion transport inhibitors on pERK1/2 levels using these cells and Western blotting (Fig. 7B). Complete removal of NaCl from the medium significantly increased the amounts of pERK1/2 in MMDD1 cells within 5 min (Fig. 7B), consistent with previous reports (8,45). Compared with control (*time 0*) and averaging all time points, pERK1/2 levels were increased by 77% (Fig. 7C). The NKCC inhibitor furosemide caused a slowly progressing, time-dependent activation (2.2-fold) of ERK1/2. Inhibiting NHE by using either EIPA or DMA (not shown) or increasing osmolality of the bathing medium from 300 to 500 mosmol/kgH_2O both had effects similar to those of salt removal with the same kinetics (Fig. 7B). The amounts of pERK1/2 increased significantly by 29% in response to EIPA and by 16% in response to hyperosmolality (Fig. 7C). In contrast, well-established techniques of either cell alkalinization (by adding 20 mM NH_4Cl to the bathing medium) (45) or cell acidification (by adding 10 μM nigericin) (30) failed to activate ERK1/2. In fact, they caused progressive reductions in pERK1/2 levels (23% reduction with NH_4Cl and 12% reduction with nigericin, Fig. 7, B and C). Effects of NH_4Cl (rapid and significant alkalinization) and nigericin (slow but marked acidification) on MMDD1 pH_i were confirmed using the pH-sensitive fluorophore BCECF as described previously (31) (Fig. 8A). Effects of EIPA and hyperosmolality on MMDD1 cell volume (both causing significant cell shrinkage) were confirmed using the calcein self-quenching technique (Fig. 8B). Mock changes of the bathing medium had no effect on pERK1/2 (not shown). All of these experiments were performed in triplicate. Equal protein loading was confirmed by probing blots with a GAPDH antibody (Fig. 7B).

Discussion

This study demonstrates for the first time that the NHE isoform NHE2, which is expressed in cells of the MD, plays an important role in the control of renin synthesis and release. Multiple lines of evidence support this conclusion. Compared with wild type, $NHE2^{-/-}$ mice exhibit increased JGA and overall renal renin content, increased intrarenal and plasma renin activities, and high levels of enzymes and signaling molecules that constitute the MD mechanism of renin release. Similarities in MAP kinase activation by pharmacological NHE inhibition and hyperosmolality-induced cell shrinkage in a MD cell line suggest that the link between reduced MD NHE2 activity and increased JGA renin signaling may be the reduction in MD cell volume.

Multiple lines of evidence suggested the significant upregulation of renal renin content in $NHE2^{-/-}$ mice, including renin immunohistochemistry, immunoblotting, and measurements of renin activity from kidney tissue and plasma (Figs. 1–3). Although renal cortical tissue immunoblotting found only a modest, 20% increase in renin content compared with the more significant changes detected by the other techniques, Western blotting is the least sensitive and JGA-specific method of all. Increased renal renin content and plasma renin activity in $NHE2^{-/-}$ mice are clearly unexpected findings. Whole animal data indicate that in contrast to NHE3-deficient mice, the $NHE2^{-/-}$ mice are not hypovolemic (19), which would have been consistent with the activation of the renin-angiotensin system. Likewise, systemic blood pressure and plasma aldosterone levels are normal in $NHE2^{-/-}$ mice (19,39). Previous studies also established that fecal salt excretion was slightly less in $NHE2^{-/-}$ mice maintained on a normal salt diet, and when switched to no-salt diet (which does not eliminate NaCl in the luminal contents because of the significant paracellular transport), both $NHE2^{-/-}$ and $NHE2^{+/+}$ mice reduced fecal salt excretion to essentially zero (19). These previous data clearly indicate that the known major NaCl-absorptive mechanisms (NHE3

and the epithelial sodium channel, ENaC) are sufficient to maintain salt absorption in the intestine, and therefore, $NHE2^{-/-}$ mice are not on a “functional” low-salt diet.

Tubuloglomerular feedback responses in $NHE2^{-/-}$ mice under control conditions are also not different from $NHE2^{+/+}$ mice (24). However, pharmacological NHE inhibition in the in vitro microperfused JGA augmented TGF responses (43). Although the present studies did not address the role of MD NHE2 in TGF, the new findings on altered MD signaling and renin content in $NHE2^{-/-}$ mice and these somewhat conflicting previous reports warrant further studies in this area. Even if there seems to be no physiological need for the inappropriately high renin synthesis in $NHE2^{-/-}$ mice, the MD mechanism of renin synthesis and release is highly active in these animals. The involvement of MD cells was suggested by the significantly increased COX-2 and mPGES expression in the cortex of $NHE2^{-/-}$ mouse kidneys, since these PGE_2-forming enzymes, at least in the renal cortex, are MD specific (6,11,15). However, other mechanisms (i.e., the baroreceptor mechanism, renal nerves, and angiotensinogen, among others) most likely compensated for the increased MD-mediated renin synthesis and release in the $NHE2^{-/-}$ mice, since there are no elevations in blood pressure and aldosterone (19,39).

The MD mechanism is one of many physiological pathways that control renin release (5,36,37,41). MD signaling that triggers renin synthesis and release starts with decreases in tubular [NaCl]. Consistent with this paradigm, no-salt diet in the present studies caused significant upregulation of renal renin content and activity in wild-type mice (Fig. 2B). However, this response was blunted in $NHE2^{-/-}$ mice, indicating that the MD feedback control of renin secretion was disrupted. These findings support the physiological importance of NHE2 in MD signaling and renin control. Previous work established that the inducible COX-2 isoform of cyclooxygenases, present in MD cells, produces prostaglandins in response to reductions in tubular [NaCl], which, upon release, acts on JG granular cells to stimulate renin release and renin synthesis (5,8,22,23,45). The underlying cellular mechanism was shown to involve MAP kinases, ERK1/2, and p38 activation that are causal in the acute release of PGE_2 as well as in the delayed rise in COX-2 mRNA and protein expression (8,9,45). It is still unclear what mechanism links MD apical ion flux to MAPK activation (8,42,45). We find it very interesting that MAP kinases are often activated by large changes in cytosolic pH and/or cell volume (12,44,45), cellular responses in which NHEs play a critical role (12,31).

The role of salt reabsorption through various NKCC2 isoforms in MD function and renin signaling is well established (7,22,23,28,29). It appears that NHE2, perhaps coupled with Cl^-/HCO_3^- anion exchangers that are expressed in MD cells (17), plays a similar role. The present studies suggest that the mechanism by which NKCC2 and NHE2 activities are coupled to the renin release signal could be MD cell volume reduction. In fact, MD cell volume is one of the important cell parameters that undergo tremendous changes when tubular salt content is altered (18,32). MD cell volume changes also appear to be maintained (18,21), a sign of inefficient cell volume regulatory mechanisms that has been attributed to the sensor function of these cells (3,18). MD cell swelling has been linked to increased tubular [NaCl]-induced afferent arteriole vasoconstriction, the TGF mechanism (32). The opposite physiological stimulus, reductions in tubular [NaCl] and MD salt reabsorption, is the classic activator of the MD renin release mechanism (5,22,23). Either Cl^- removal or furosemide administration that triggers renin release (22,23) can cause significant MD cell shrinkage (13,18). The present studies confirmed that NHE inhibition with EIPA also causes MD cell shrinkage (Fig. 8B). Thus MD cell volume seems to be ideally tracking the alterations in tubular fluid composition and these opposing physiological mechanisms. It has been established that both NKCC2 and NHE2 are involved in MD apical salt entry with an estimated 80:20 ratio (3,33). Consistent with this is the intriguing present finding that

furosemide, an inhibitor of NKCC2, caused an approximately fourfold more intense activation of ERK1/2 within 15 min than did EIPA, a blocker of NHE2 (Fig. 7, B and C). Although NKCC2 is the primary player, the contribution of NHE2 to cell volume still appears to be significant (Fig. 8B). Although low MD cell volume is one possible mechanism by which NHE2 activity is coupled to renin synthesis and release, other mechanisms such as the direct interaction between NHE2 and MAP kinases or other signaling molecules cannot be ruled out. Also, it should be noted that the magnitude of change in medium osmolality (from 300 to 500 mosmol/kgH_2O) applied in the present cell culture experiments is well within the range used for MD cells by others (13,18,21).

MMDD1 cells were reported to produce cell acidification upon bath Na^+ removal, a clear sign of plasma membrane Na^+/H^+ exchange (45). In addition, the present studies confirmed that MMDD1 cells express NHE2 (Fig. 7A), suggesting that these cells are useful to study NHE2-dependent MD cell signaling mechanisms. Regulation of pH_i is another key function of NHEs (31), and MD NHE2 activity, based on tubular salt content, has been shown to cause large changes in MD pH_i (10,31). Low tubular [NaCl] is associated with acidic MD pH_i, and cell acidification is known to activate MAP kinases in some cell types (12,30). However, direct and salt-independent cell acidification by nigericin in the present studies failed to activate ERK1/2, a result clearly different from the effect of NHE inhibition (Fig. 7, B and C). Thus it seems unlikely that reduced NHE2 activity generates the renin signal through cell acidification. However, it is possible that low pH_i acts on molecular targets other than ERK1/2.

In contrast to previous work (8,45) that failed to detect Na^+ removal-dependent activation of MAP kinases in cells of the MD and cortical thick ascending limb, the present studies found significant and rapid phosphorylation of ERK1/2 in response to NHE inhibition. A possible explanation for these results could be the use of different experimental salt solutions. In previous work, the lowest [Na^+] was 68 mM (44) or 26 mM (8), or in other words, only partial Na^+ removal was used. Given that the resting [Na^+] in MD cells is in the 30 mM range (33), these concentrations most likely did not significantly alter NHE activity. The present studies used pharmacological inhibitors (EIPA and DMA) at a concentration that provides maximal inhibition of MD NHE2 (31,43). Significant and rapid activation of ERK1/2 was observed in these experiments consistent with the role of ERK1/2 in acute PGE_2 release (8,45). Although the present cell culture studies showed acute and transient activations of ERK1/2 in response to various stimuli (Fig. 7B), chronic activation of ERK1/2 was evident in the native tissue, in MD cells of $NHE2^{-/-}$ kidneys (Fig. 6), consistent with the chronic stimulation of COX-2 and JGA renin in $NHE2^{-/-}$ mice (Fig. 5).

In summary, the present studies identified another element of the MD salt-sensing mechanism that is important in the control of renin synthesis and release. Reductions in MD NHE2 activity lead to the phosphorylation of MAP kinases ERK1/2 and the activation of the PGE_2 synthetic machinery including COX-2 and mPGES. NHE2 activity may be linked to renin signaling via reductions in MD cell volume. Because of the importance of renin and other elements of the renin-angiotensin-aldosterone system in many different health and disease conditions, NHE2 is a potential new target of therapeutic interventions.

Acknowledgments

GRANTS: This work was supported by National Institute of Diabetes and Digestive and Kidney Diseases Grant DK-64324 (to J. Peti-Peterdi), grants from Institut National de la Sante et de la Recherche Medicale (to D. Eladari and R. Chambrey), and Hungarian Research Grant OTKA AT 048767 (to L. Rosivall).

References

1. Aronson PS. Ion exchangers mediating NaCl transport in the renal proximal tubule. Cell Biochem Biophys. 2002; 36:147–53. [PubMed: 12139400]
2. Barajas L. Anatomy of the juxtaglomerular apparatus. Am J Physiol Renal Fluid Electrolyte Physiol. 1979; 237:F333–F343.
3. Bell PD, Lapointe JY, Peti-Peterdi J. Macula densa cell signaling. Annu Rev Physiol. 2003; 65:481–500. [PubMed: 12524458]
4. Biemesderfer D, Rutherford PA, Nagy T, Pizzonia JH, Abu-Alfa AK, Aronson PS. Monoclonal antibodies for high-resolution localization of NHE3 in adult and neonatal rat kidney. Am J Physiol Renal Physiol. 1997; 273:F289–F299.
5. Briggs JP, Lorenz JN, Weihprecht H, Schnermann J. Macula densa control of renin secretion. Renal Physiol Biochem. 1991; 14:164–174. [PubMed: 1708903]
6. Campean V, Theilig F, Paliege A, Breyer M, Bachmann S. Key enzymes for renal prostaglandin synthesis: site-specific expression in rodent kidney (rat, mouse). Am J Physiol Renal Physiol. 2003; 285:F19–F32. [PubMed: 12657565]
7. Castrop H, Lorenz JN, Hansen PB, Friis U, Mizel D, Oppermann M, Jensen BL, Briggs J, Skott O, Schnermann J. Contribution of the basolateral isoform of the Na-K-2Cl^- cotransporter (NKCC1/BSC2) to renin secretion. Am J Physiol Renal Physiol. 2005; 289:F1185–F1192. [PubMed: 16106034]
8. Cheng HF, Wang JL, Zhang MZ, McKanna JA, Harris RC. Role of p38 in the regulation of renal cortical cyclooxygenase-2 expression by extracellular chloride. J Clin Invest. 2000; 106:681–688. [PubMed: 10974021]
9. Cheng HF, Harris RC. Cyclooxygenase-2 expression in cultured cortical thick ascending limb of Henle increases in response to decreased extracellular ionic content by both transcriptional and post-transcriptional mechanisms. Role of p38-mediated pathways. J Biol Chem. 2002; 277:45638–45643. [PubMed: 12237297]
10. Fowler BC, Chang YS, Laamarti A, Higdon M, Lapointe JY, Bell PD. Evidence for apical sodium proton exchange in macula densa cells. Kidney Int. 1995; 47:746–751. [PubMed: 7752573]
11. Fuson AL, Komlosi P, Unlap TM, Bell PD, Peti-Peterdi J. Immunolocalization of a microsomal prostaglandin E synthase in rabbit kidney. Am J Physiol Renal Physiol. 2003; 285:F558–F564. [PubMed: 12746259]
12. Gillis D, Shrode LD, Krump E, Howard CM, Rubie EA, Tibbles LA, Woodgett J, Grinstein S. Osmotic stimulation of the Na^+/H^+ exchanger NHE1: relationship to the activation of three MAPK pathways. J Membr Biol. 2001; 181:205–214. [PubMed: 11420607]
13. González E, Salomonsson M, Müller-Suur C, Persson AE. Measurements of macula densa cell volume changes in isolated and perfused rabbit cortical thick ascending limb. I. Isosmotic and anisosmotic cell volume changes. Acta Physiol Scand. 1988; 133:149–157. [PubMed: 3227911]
14. Hamann S, Herrera-Perez JJ, Bundgaard M, Alvarez-Leefmans FJ, Zeuthen T. Water permeability of Na^+-K^+-2Cl^- cotransporters in mammalian epithelial cells. J Physiol. 2005; 568:123–135. [PubMed: 16020454]
15. Harris RC, Breyer MD. Physiological regulation of cyclooxygenase-2 in the kidney. Am J Physiol Renal Physiol. 2001; 281:F1–F11. [PubMed: 11399641]
16. Kang JJ, Toma I, Sipos A, McCulloch F, Peti-Peterdi J. Imaging the renin-angiotensin system: an important target of anti-hypertensive therapy. Adv Drug Delivery Res. 2006; 58:824–833.
17. Komlosi P, Frische S, Fuson AL, Fintha A, Zsembery A, Peti-Peterdi J, Bell PD. Characterization of basolateral chloride/bicarbonate exchange in macula densa cells. Am J Physiol Renal Physiol. 2005; 288:F380–F386. [PubMed: 15479854]
18. Komlosi P, Fintha A, Bell PD. Unraveling the relationship between macula densa cell volume and luminal solute concentration/osmolality. Kidney Int. 2006; 70:865–871. [PubMed: 16820788]
19. Ledoussal C, Lorenz JN, Nieman ML, Soleimani M, Schultheis PJ, Shull GE. Renal salt wasting in mice lacking NHE3 Na^+/H^+ exchanger but not in mice lacking NHE2. Am J Physiol Renal Physiol. 2001; 281:F718–F727. [PubMed: 11553519]

20. Liu R, Carretero OA, Ren Y, Garvin JL. Increased intracellular pH at the macula densa activates nNOS during tubuloglomerular feedback. Kidney Int. 2005; 67:1837–1843. [PubMed: 15840031]
21. Liu R, Persson AE. Simultaneous changes of cell volume and cytosolic calcium concentration in macula densa cells caused by alterations of luminal NaCl concentration. J Physiol. 2005; 563:895–901. [PubMed: 15661823]
22. Lorenz JN, Weihprecht H, Schnermann J, Skott O, Briggs JP. Renin release from isolated juxtaglomerular apparatus depends on macula densa chloride transport. Am J Physiol Renal Fluid Electrolyte Physiol. 1991; 260:F486–F493.
23. Lorenz JN, Greenberg SG, Briggs JP. The macula densa mechanism for control of renin secretion. Semin Nephrol. 1993; 13:531–542. [PubMed: 8278686]
24. Lorenz JN, Dostanic-Larson I, Shull GE, Lingrel JB. Ouabain inhibits tubuloglomerular feedback in mutant mice with ouabain-sensitive alpha1 Na,K-ATPase. J Am Soc Nephrol. 2006; 17:2457–2463. [PubMed: 16870707]
25. McCulloch F, Chambrey R, Eladari D, Peti-Peterdi J. Localization of connexin 30 in the luminal membrane of cells in the distal nephron. Am J Physiol Renal Physiol. 2005; 289:F1304–F1312. [PubMed: 16077080]
26. Menard J, Catt KJ. Measurement of renin activity, concentration and substrate in rat plasma by radioimmunoassay of angiotensin I. Endocrinology. 1972; 90:422–430. [PubMed: 4109649]
27. Norling LL, Gomez RA, Inagami T. Characterization of a synthetic peptide antibody recognizing rat kidney renin and prorenin. Clin Nephrol. 1995; 43:232–236. [PubMed: 7541738]
28. Oppermann M, Mizel D, Kim SM, Chen L, Faulhaber-Walter R, Huang Y, Li C, Deng C, Briggs J, Schnermann J, Castrop H. Renal function in mice with targeted disruption of the A isoform of the Na-K-2Cl co-transporter. J Am Soc Nephrol. 2007; 18:440–448. [PubMed: 17215439]
29. Oppermann M, Mizel D, Huang G, Li C, Deng C, Theilig F, Bachmann S, Briggs J, Schnermann J, Castrop H. Macula densa control of renin secretion and preglomerular resistance in mice with selective deletion of the B isoform of the Na,K,2Cl co-transporter. J Am Soc Nephrol. 2006; 17:2143–2152. [PubMed: 16807402]
30. Parfenova H, Haffner J, Leffler CW. Phosphorylation-dependent stimulation of prostanoid synthesis by nigericin in cerebral endothelial cells. Am J Physiol Cell Physiol. 1999; 277:C728–C738.
31. Peti-Peterdi J, Chambrey R, Bebok Z, Biemesderfer D, St John PL, Abrahamson DR, Warnock DG, Bell PD. Macula densa Na^+/H^+ exchange activities mediated by apical NHE2 and basolateral NHE4 isoforms. Am J Physiol Renal Physiol. 2000; 278:F452–F463. [PubMed: 10710550]
32. Peti-Peterdi J, Morishima S, Bell PD, Okada Y. Two-photon excitation fluorescence imaging of the living juxtaglomerular apparatus. Am J Physiol Renal Physiol. 2002; 283:F197–F201. [PubMed: 12060602]
33. Peti-Peterdi J, Bebok Z, Lapointe JY, Bell PD. Novel regulation of cell $[Na^+]$ in macula densa cells: apical Na^+ recycling by H-K-ATPase. Am J Physiol Renal Physiol. 2002; 282:F324–F329. [PubMed: 11788447]
34. Peti-Peterdi J, Komlosi P, Fuson AL, Guan Y, Schneider A, Qi Z, Redha R, Rosivall L, Breyer MD, Bell PD. Luminal NaCl delivery regulates basolateral PGE_2 release from macula densa cells. J Clin Invest. 2003; 112:76–82. [PubMed: 12840061]
35. Peti-Peterdi J, Fintha A, Fuson AL, Tousson A, Chow RH. Real-time imaging of renin release in vitro. Am J Physiol Renal Physiol. 2004; 287:F329–F335. [PubMed: 15082450]
36. Schnermann, J.; Briggs, J. Function of the juxtaglomerular apparatus: local control of glomerular hemodynamics. In: Seldin, DW.; Giebisch, G., editors. The Kidney. New York: Raven; 1985. p. 669-697.
37. Schnermann J. Juxtaglomerular cell complex in the regulation of renal salt excretion. Am J Physiol Regul Integr Comp Physiol. 1998; 274:R263–R279.
38. Schnermann J, Levine DZ. Paracrine factors in tubuloglomerular feedback: adenosine, ATP, and nitric oxide. Annu Rev Physiol. 2003; 65:501–529. [PubMed: 12208992]
39. Schultheis PJ, Clarke LL, Meneton P, Harline M, Boivin GP, Stemmermann G, Duffy JJ, Doetschman T, Miller ML, Shull GE. Targeted disruption of the murine Na^+/H^+ exchanger

isoform 2 gene causes reduced viability of gastric parietal cells and loss of net acid secretion. J Clin Invest. 1998; 101:1243–1253. [PubMed: 9502765]

40. Schweda F, Klar J, Narumiya S, Nusing RM, Kurtz A. Stimulation of renin release by prostaglandin E_2 is mediated by EP2 and EP4 receptors in mouse kidneys. Am J Physiol Renal Physiol. 2004; 287:F427–F433. [PubMed: 15113745]
41. Schweda F, Friis U, Wagner C, Skott O, Kurtz A. Renin release. Physiology (Bethesda). 2007; 22:310–319. [PubMed: 17928544]
42. Thomson SC, Blantz RC. Ions and signal transduction in the macula densa. J Clin Invest. 2000; 106:633–635. [PubMed: 10974015]
43. Wang H, Carretero OA, Garvin JL. Inhibition of apical Na^+/H^+ exchangers on the macula densa cells augments tubuloglomerular feedback. Hypertension. 2003; 41:688–691. [PubMed: 12623980]
44. Yang T, Huang Y, Heasley LE, Berl T, Schnermann JB, Briggs JP. MAPK mediation of hypertonicity-stimulated cyclooxygenase-2 expression in renal medullary collecting duct cells. J Biol Chem. 2000; 275:23281–23286. [PubMed: 10930430]
45. Yang T, Park JM, Arend L, Huang Y, Topaloglu R, Pasumarthy A, Praetorius H, Spring K, Briggs JP, Schnermann J. Low chloride stimulation of prostaglandin E_2 release and cyclooxygenase-2 expression in a mouse macula densa cell line. J Biol Chem. 2000; 275:37922–37929. [PubMed: 10982805]

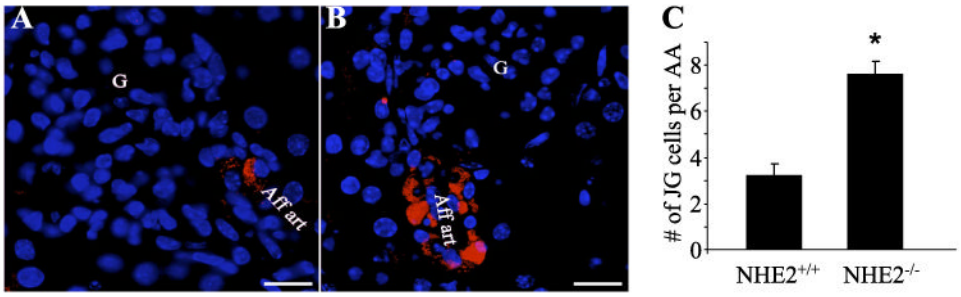

Fig. 1.

Renin immunofluorescence (red) in wild-type ($NHE2^{+/+}$; *A*) and Na^+/H^+ exchanger isoform NHE2 knockout ($NHE2^{-/-}$) mouse kidneys (*B*). Nuclei are blue. G, glomerulus; Aff art, afferent arteriole. Bar, 20 μm. *C*: summary of the number of renin-expressing juxtaglomerular (JG) cells per afferent arteriole (AA) in $NHE2^{+/+}$ and $NHE2^{-/-}$ mouse kidneys. $*P < 0.05$.

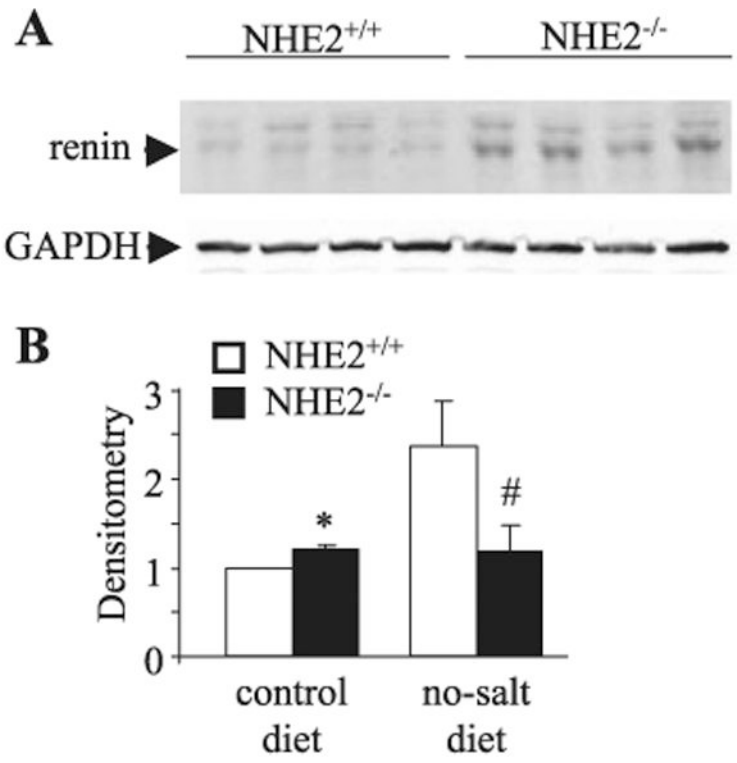

Fig. 2.

Immunoblotting analysis of renal cortical renin content in $NHE2^{+/+}$ and $NHE2^{-/-}$ mice. Four representative samples are shown from each group on normal salt diet (*A*). The band around 50 kDa, typical for renin, was used for densitometry analysis (*B*). Data were normalized to wild-type mice on control diet. GAPDH blot was used as a loading control. Renin protein content of the renal cortex was significantly increased in $NHE2^{-/-}$ compared with $NHE2^{+/+}$ mice fed normal salt diet (*$P < 0.05$). No-salt diet for 1 wk significantly increased renin content in $NHE2^{+/+}$ mice, but this response was blunted in $NHE2^{-/-}$ mice. #$P < 0.05$, low-salt $NHE2^{+/+}$ vs. low-salt $NHE2^{-/-}$ ($n = 3$ each).

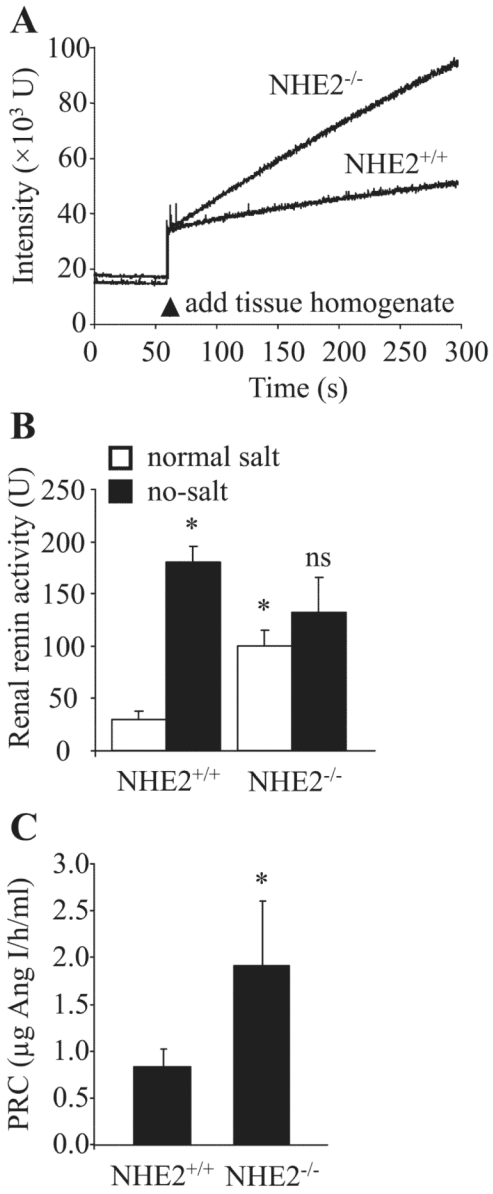

Fig. 3.

Renin activity in the renal cortex and plasma in NHE2$^{+/+}$ and NHE2$^{-/-}$ mice. Representative recordings (*A*) and summary data (*B*) of tissue renin activity measured in real-time using a fluorescence resonance energy transfer (FRET)-based fluorogenic renin substrate. The initial rate of the increase in fluorescence after the addition of tissue homogenate (*A*) was analyzed as an index of ANG I generation (renin activity; *B*). Renin activity was significantly higher in NHE2$^{-/-}$ mice compared with NHE2$^{+/+}$ mice on normal salt intake (n = 5 for NHE2$^{+/+}$ and n = 6 for NHE2$^{-/-}$). No-salt diet for 1 wk increased renal tissue renin activity in NHE2$^{+/+}$ mice, but this response was significantly blunted in NHE2$^{-/-}$ mice. *P < 0.01 compared with NHE2$^{+/+}$ mice on normal salt diet; ns, not significantly different from NHE2$^{-/-}$ mice on normal diet (n = 3 each group). *C*: plasma renin concentration (PRC) was measured by radioimmunoassay of ANG I generated in the presence of an excess of rat angiotensinogen. *P < 0.05 (n = 8 for NHE2$^{+/+}$ and n = 11 for NHE2$^{-/-}$).

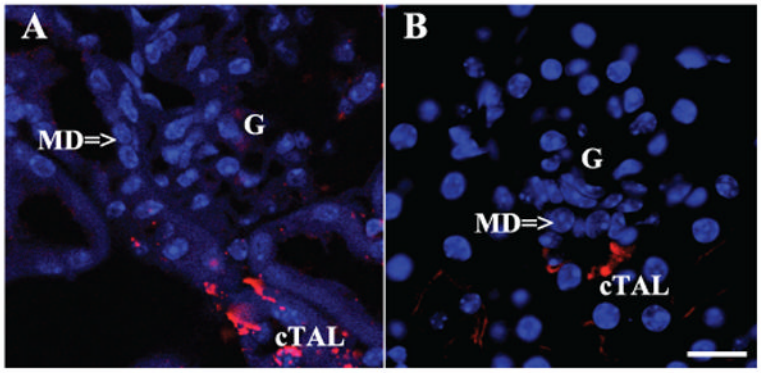

Fig. 4.

NHE3 immunofluorescence (red) in NHE2$^{+/+}$ (*A*) and NHE2$^{-/-}$ mouse kidney (*B*). Cells of the cortical thick ascending limb (cTAL) are positive for NHE3 at the apical membrane, whereas the adjacent macula densa (MD) cells are devoid of NHE3 staining in both genotypes. Nuclei are blue. Bar, 20 μm.

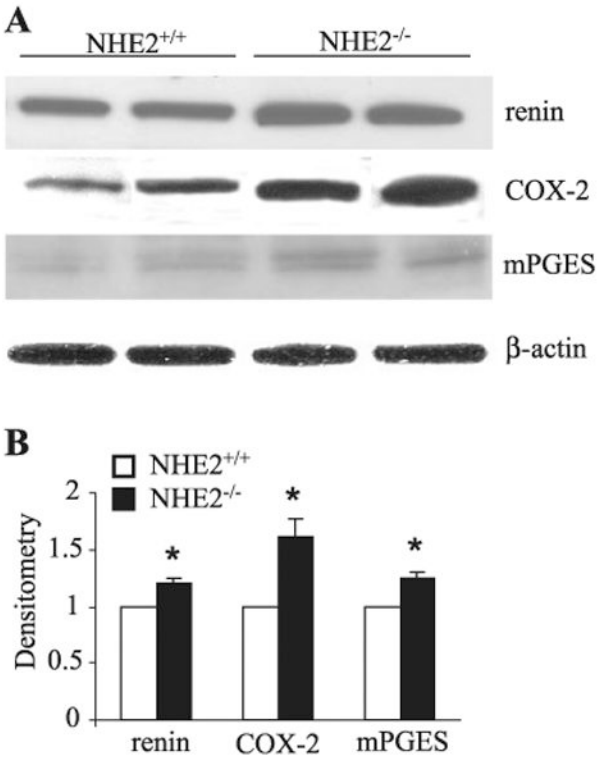

Fig. 5.

Parallel analysis of renin, cyclooxygenase-2 (COX-2), and microsomal prostaglandin E synthase (mPGES) expression in renal cortical homogenates from $NHE2^{+/+}$ and $NHE2^{-/-}$ mice using immunoblotting. *A*: 2 representative samples are shown from each group. Bands were detected at the expected sizes for renin, COX-2, and mPGES at 50, 72, and 16 kDa, respectively. Significantly increased levels of renin, COX-2, and mPGES were observed in $NHE2^{-/-}$ compared with $NHE2^{+/+}$ mice. Equal protein loading was confirmed by probing blots with a β-actin antibody. *B:* summary of the densitometry analysis. Data are normalized to the wild-type group. $*P < 0.05$.

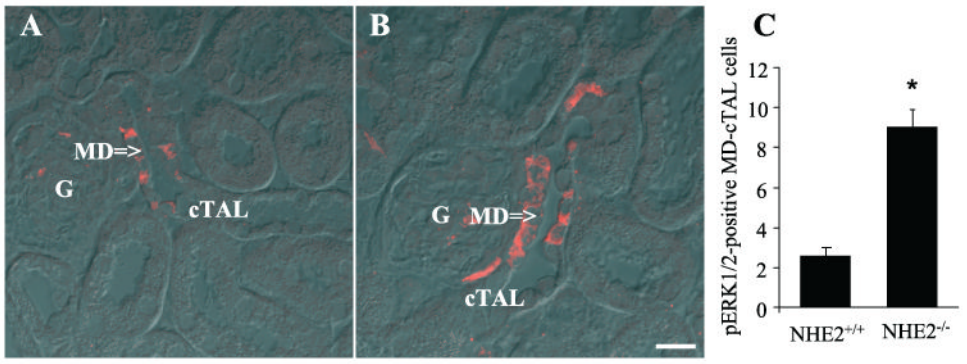

Fig. 6.

Activated ERK1/2 immunofluorescence (red) in NHE2$^{+/+}$ (*A*) and NHE2$^{-/-}$ mouse kidneys (*B*). Differential interference-contrast overlay is shown to visualize kidney structure. Bar, 20 μm. *C*: summary of the number of phosphorylated pERK1/2-positive cells per JG apparatus (JGA) in NHE2$^{+/+}$ and NHE2$^{-/-}$ kidneys. *$P < 0.05$. The number of JGAs analyzed was $n = 7$ in each group from 3 separate samples each.

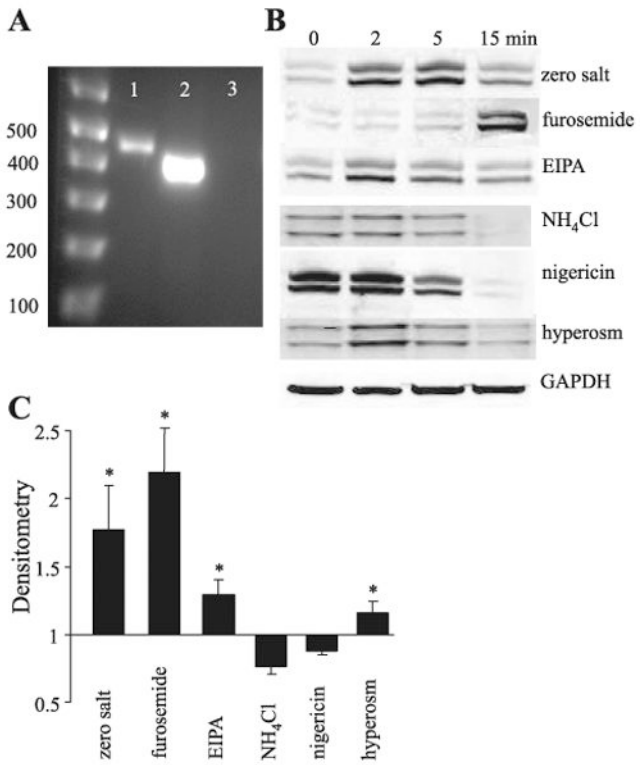

Fig. 7.

Studies using cultured mouse macula densa-derived (MMDD1) cells. *A*: detection of NHE2 mRNA in MMDD1 cells. mRNA isolated from MMDD1 cells was amplified by RT-PCR to detect NHE2 (*lane 1*) and β-actin (*lane 2*). Bands were observed approximately at the predicted sizes of 455 and 350 bp for NHE2 and β-actin, respectively. Lack of band in *lane 3* ($NHE2^{-/-}$ mouse whole kidney DNA) confirmed the specificity of NHE2 primers. *B*: immunoblot analysis of pERK1/2 in MMDD1 cells. Both the removal of NaCl and the addition of ethylisopropyl amiloride (EIPA; 100 μM), a Na^+/H^+ exchange inhibitor, activated ERK1/2 within 5 min after treatment. Furosemide caused a slowly progressing, time-dependent activation of ERK1/2. Both cell alkalinization with NH_4Cl (20 mM) and cell acidification with nigericin (10 μM) reduced or did not change pERK1/2 levels. Similar to NaCl removal and EIPA, increasing medium osmolality to 500 mosmol/kgH_2O with mannitol significantly increased pERK1/2 levels. Bands were detected at the expected sizes for ERK1/2 at 44 and 42 kDa, respectively. Equal protein loading was confirmed by probing blots with a GAPDH antibody. All experiments were performed in triplicate. *C*: summary of the densitometry analysis. Data are normalized to the value at *time 0*, and all time points (2, 5, and 15 min) are included in data analysis. *$P < 0.05$, increase compared with *time 0* (n = 9 each group).

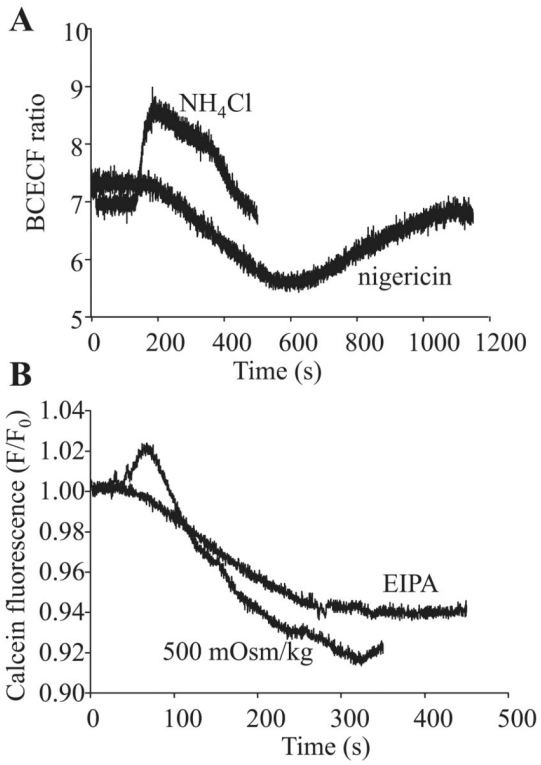

Fig. 8.

Representative recordings of the changes in MMDD1 cell pH (*A*) or volume (*B*) caused by the experimental maneuvers employed in the MAP kinase study. *A*: addition of NH_4Cl (20 mM) to MMDD1 cells in Krebs-Ringer solution caused rapid and significant increases in BCECF ratio, indicating cell alkalinization. Addition of nigericin (10 μM) caused cell acidification. After the BCECF ratio stabilized during the experiments, the superfusate was changed back to the control Krebs-Ringer solution (at 250 s for NH_4Cl and at 600 s for nigericin) for pH recovery. *B*: normalized calcein fluorescence (F/F_0) decreased similarly by increasing medium osmolality to 500 mosmol/kgH_2O (isosmotic Krebs-Ringer solution with added mannitol) or adding 100 μM EIPA, indicating significant MMDD1 cell shrinkage under these conditions. All experiments were performed in triplicate.